

---

# CMS Physics Analysis Summary

---

Contact: cms-pag-conveners-susy@cern.ch

2011/07/26

## Search for supersymmetry in all-hadronic events with $\alpha_T$

The CMS Collaboration

### Abstract

An update of the search for supersymmetry in events with jets and missing transverse energy, based on the analysis in Ref. [1], is presented. The results are based on a data sample of  $1.1 \text{ fb}^{-1}$  of integrated luminosity recorded at  $\sqrt{s} = 7 \text{ TeV}$ . In this search, the variable  $\alpha_T$  is used as the main discriminator between events with real and fake missing transverse energy, and no excess of events over the Standard Model expectation is found. Given this agreement, exclusion limits in the parameter space of the constrained minimal supersymmetric model are set. In this model, squark and gluino masses of  $1.1 \text{ TeV}$  are excluded for values of the common scalar mass at the GUT scale  $m_0 < 0.5 \text{ TeV}$ .



## Contents

1	Introduction	2
2	Trigger, Event Selection and Analysis	2
2.1	Data to Monte Carlo Comparison for Analysis Variables	4
2.2	$H_T$ Dependence of $R_{\alpha_T}$	5
2.3	Estimation of Background from $t\bar{t}$ and $W + \text{Jets}$ Events using a Muon Control Sample	7
2.4	Estimation of Background from $Z \rightarrow \nu\bar{\nu} + \text{Jets}$ from Photon + Jets Events	8
2.5	Background Cross-Check: Estimation of $W \rightarrow \mu\nu + \text{Jets}$ Events from Photon + Jets Events	8
3	Systematic Uncertainties on Signal Efficiency	10
4	Framework for Statistical Interpretation	11
4.1	Hadronic Selection	11
4.2	Testing the Goodness-of-Fit of the SM-only Hypothesis	11
4.3	Testing specific SUSY Models	11
4.4	Electroweak Background Constraints	12
4.5	$H_T$ Evolution Method	12
4.6	Likelihood Model	13
5	Final Results	13
6	Summary	14

## 1 Introduction

In this note we present an update of the search for a missing energy signature in dijet and multijet events using the  $\alpha_T$  variable. The current results are based on  $1.1 \text{ fb}^{-1}$  of LHC data recorded in 2011 at a centre-of-mass energy of  $\sqrt{s} = 7 \text{ TeV}$ .

The presented search concentrates on event topologies in which heavy new particles are pair-produced in a proton-proton collision and where at the end of their decay chain a weakly interacting massive particle (WIMP) is produced. The latter remains undetected, thus leading to a missing energy signature. In the case of SUSY, squarks and gluinos could be the heavy particles while the lightest (and stable) neutralino  $\chi_1^0$  is the WIMP candidate. Although this search is carried out in the context of SUSY, the results are applicable to other New Physics scenarios as the missing energy signature is common to many models, e.g., Extra Dimensions and Little Higgs models.

To interpret the results, a simplified and practical model of SUSY-breaking, the constrained minimal supersymmetric extension of the standard model (CMSSM) [2, 3], is used. The CMSSM is described by five parameters: the universal scalar and gaugino mass parameters ( $m_0$  and  $m_{1/2}$ , respectively), the universal trilinear soft SUSY breaking parameter  $A_0$ , and two low-energy parameters, the ratio of the two vacuum expectation values of the two Higgs doublets,  $\tan \beta$ , and the sign of the Higgs mixing parameter,  $\text{sign}(\mu)$ . Throughout this note, two CMSSM parameter sets, referred to as LM4 and LM6 [4] and not excluded by the 2010 analysis [1], are used to illustrate possible CMSSM yields. The parameter values defining LM4 (LM6) are  $m_0 = 210 \text{ GeV}$ ,  $m_{1/2} = 285 \text{ GeV}$ , ( $m_0 = 85 \text{ GeV}$ ,  $m_{1/2} = 400 \text{ GeV}$ ) and  $A_0 = 0$ ,  $\tan \beta = 10$ , and  $\text{sign}(\mu) > 0$  for both points.

Events with  $n$  high- $p_T$  hadronic jets are studied and the missing transverse momentum is inferred through the measured jet momenta via the kinematic variable  $\alpha_T$ , which was initially inspired by Ref. [5]. The analysis follows closely Ref. [1] and two previous Physics Analysis Summaries [6, 7]. The main difference with respect to Ref. [1] is that rather than defining a specific signal region, we now search for an excess of events in data over the Standard Model expectation over the entire  $H_T = \sum_{i=1}^n E_T^{\text{jet}_i}$  range above  $275 \text{ GeV}$ . This approach is complementary to the searches carried out in Refs. [8] and [9]. The dominant background which arises from QCD multi-jets can be suppressed significantly with a selection requirement on the  $\alpha_T$  variable. To estimate the remaining backgrounds we make use of data control samples. These are a  $\mu + \text{jets}$  sample for the background from  $W + \text{jets}$  and  $t\bar{t}$  events, and a photon+jets sample to determine the background from  $Z \rightarrow \nu\bar{\nu}$  events.

## 2 Trigger, Event Selection and Analysis

The trigger strategy has changed from that of the 2010 analysis [1], where a pure  $H_T$  trigger was used to collect both the signal and the control samples. With the increase in instantaneous luminosity seen in 2011, the  $H_T$  thresholds of these triggers are too high for the analysis. In contrast to 2010, the High Level Trigger has moved to using energy corrected jets to calculate  $H_T$  which results in a much steeper trigger efficiency curve as a function of  $H_T$ . To ensure that the trigger is fully efficient with respect to the final event selection, the offline  $H_T$  bin edges have been shifted up by  $25 \text{ GeV}$  with respect to the online values. The analysis therefore uses the following  $H_T$  binning:  $275, 325, 375, 475, 575, 675, 775$ , and  $> 875 \text{ GeV}$ .

To select candidate events with jets + missing transverse energy, cross-object triggers between  $H_T$  and  $\cancel{H}_T = |\vec{H}_T| = |\sum_{i=1}^n \vec{p}_T^{\text{jet}_i}|$  are used. Due to evolving trigger thresholds on the  $\cancel{H}_T$  part

of the trigger over the period of data collection, a small inefficiency of  $0.99^{+0.01}_{-0.02}$  is encountered in the lowest  $H_T = 275$  GeV bin and corrected for. In the  $H_T = 325$  GeV (375 GeV) bins, the trigger is fully efficient with a statistical uncertainty of 3.4% (3.2%).

A suite of prescaled  $H_T$  triggers is used to select events which stem mainly in QCD multi-jet production. A photon control sample to constrain the background from  $Z \rightarrow \nu\bar{\nu}$  events is selected with a single object photon trigger.

The analysis follows closely Ref. [1]. Events with two or more high- $p_T$  jets, reconstructed using the anti- $k_T$  algorithm [10] with a size parameter of 0.5 are selected. Jets are required to have  $E_T > 50$  GeV,  $|\eta| < 3$  and to pass jet identification criteria [11] designed to reject spurious signals and noise in the calorimeters. The pseudorapidity of the jet with the highest  $E_T$  (leading jet) is required to be within  $|\eta| < 2.5$ , and the transverse energy of each of the two leading jets must exceed 100 GeV.

Events with jets passing the  $E_T$  threshold but not satisfying the jet identification criteria or the  $\eta$  acceptance requirement are vetoed, as this deposited energy is not accounted for in the event kinematics. Similarly, events in which an isolated lepton (electron or muon) with  $p_T > 10$  GeV is identified are rejected to suppress events with genuine missing energy from neutrinos. The electron and muon selection requirements are described in [12] and [13], respectively. Furthermore, to select a pure multi-jet topology, events are vetoed in which an isolated photon [14] with  $p_T > 25$  GeV is found.

Events are required to satisfy  $H_T > 275$  GeV. As the main discriminator against QCD multijet production the variable  $\alpha_T$ , defined for di-jet events as:

$$\alpha_T = \frac{E_T^{\text{jet}2}}{M_T} = \frac{E_T^{\text{jet}2}}{\sqrt{\left(\sum_{i=1}^2 E_T^{\text{jet}_i}\right)^2 - \left(\sum_{i=1}^2 p_x^{\text{jet}_i}\right)^2 - \left(\sum_{i=1}^2 p_y^{\text{jet}_i}\right)^2}},$$

is used and events are required to have  $\alpha_T > 0.55$ . In events with jet multiplicity  $n > 2$ , two pseudo-jets are formed following Ref. [1] and Eq. 2 is applied to the pseudo-jets.

To protect against multiple jets failing the  $E_T > 50$  GeV selection requirement, the jet-based estimate of the missing transverse energy,  $\cancel{H}_T$ , is compared to the calorimeter tower-based estimate,  $\cancel{E}_T^{\text{calo}}$ , and events with  $R_{\text{miss}} = \cancel{H}_T / \cancel{E}_T^{\text{calo}} > 1.25$  are rejected.

Finally, to protect against severe energy losses, events with significant jet mismeasurements caused by masked regions in the ECAL (which amount to about 1% of the ECAL channel count), or by missing instrumentation in the barrel-endcap gap, are removed with the following procedure. The jet-based estimate of the missing transverse energy,  $\cancel{H}_T$ , is used to identify jets most likely to have given rise to the  $\cancel{H}_T$  as those whose momentum is closest in  $\phi$  to the total  $\vec{\cancel{H}}_T$  which results after removing them from the event. The azimuthal distance between this jet and the recomputed  $\cancel{H}_T$  is referred to as  $\Delta\phi^*$  in what follows. Events with  $\Delta\phi^* < 0.5$  are rejected if the distance in the  $(\eta, \phi)$  plane between the selected jet and the closest masked ECAL region,  $\Delta R_{\text{ECAL}}$ , is smaller than 0.3. Similarly, events are rejected if the jet points within 0.3 in  $\eta$  of the ECAL barrel-endcap gap at  $|\eta| = 1.5$ .

To increase the sensitivity to higher-mass states, we carry out a shape analysis over the entire  $H_T > 275$  GeV region. This requires that the Standard Model background estimation methods which are based on data control samples, provide an estimate of the background for each of the  $H_T$  bins in the signal region with  $H_T > 275$  GeV. The background estimation methods based on

data control samples as used in Ref. [1] were explicitly designed with this use-case in mind. In the following, the results for the different background prediction methods are presented when splitting the signal region into 8 bins, as defined in Table 1.

The results of this selection are documented in Table 1 and comparisons between Data and Monte Carlo (MC) simulation for control variables are shown in Section 2.1.

Table 1: Definition of the  $H_T$  bins and the corresponding  $p_T$  thresholds for the leading, second, and all remaining jets in the event; the number of events passing and failing the  $\alpha_T$  cut and the resulting  $R_{\alpha_T}$  value, for  $1.1 \text{ fb}^{-1}$  of data collected in 2011.

$H_T$ Bin (GeV)	275–325	325–375	375–475	475–575
$p_T^{\text{leading}}$ (GeV)	73	87	100	100
$p_T^{\text{second}}$ (GeV)	73	87	100	100
$p_T^{\text{other}}$ (GeV)	37	43	50	50
$\alpha_T > 0.55$	782	321	196	62
$\alpha_T < 0.55$	$5.73 \cdot 10^7$	$2.36 \cdot 10^7$	$1.62 \cdot 10^7$	$5.12 \cdot 10^6$
$R_{\alpha_T} (10^{-5})$	$1.36 \pm 0.05_{\text{stat}}$	$1.36 \pm 0.08_{\text{stat}}$	$1.21 \pm 0.09_{\text{stat}}$	$1.21 \pm 0.15_{\text{stat}}$
$H_T$ Bin (GeV)	575–675	675–775	775–875	$875-\infty$
$p_T^{\text{leading}}$ (GeV)	100	100	100	100
$p_T^{\text{second}}$ (GeV)	100	100	100	100
$p_T^{\text{other}}$ (GeV)	50	50	50	50
$\alpha_T > 0.55$	21	6	3	1
$\alpha_T < 0.55$	$1.78 \cdot 10^6$	$6.89 \cdot 10^5$	$2.90 \cdot 10^5$	$2.60 \cdot 10^5$
$R_{\alpha_T} (10^{-5})$	$1.18 \pm 0.26_{\text{stat}}$	$0.87 \pm 0.36_{\text{stat}}$	$1.03 \pm 0.60_{\text{stat}}$	$0.39 \pm 0.52_{\text{stat}}$

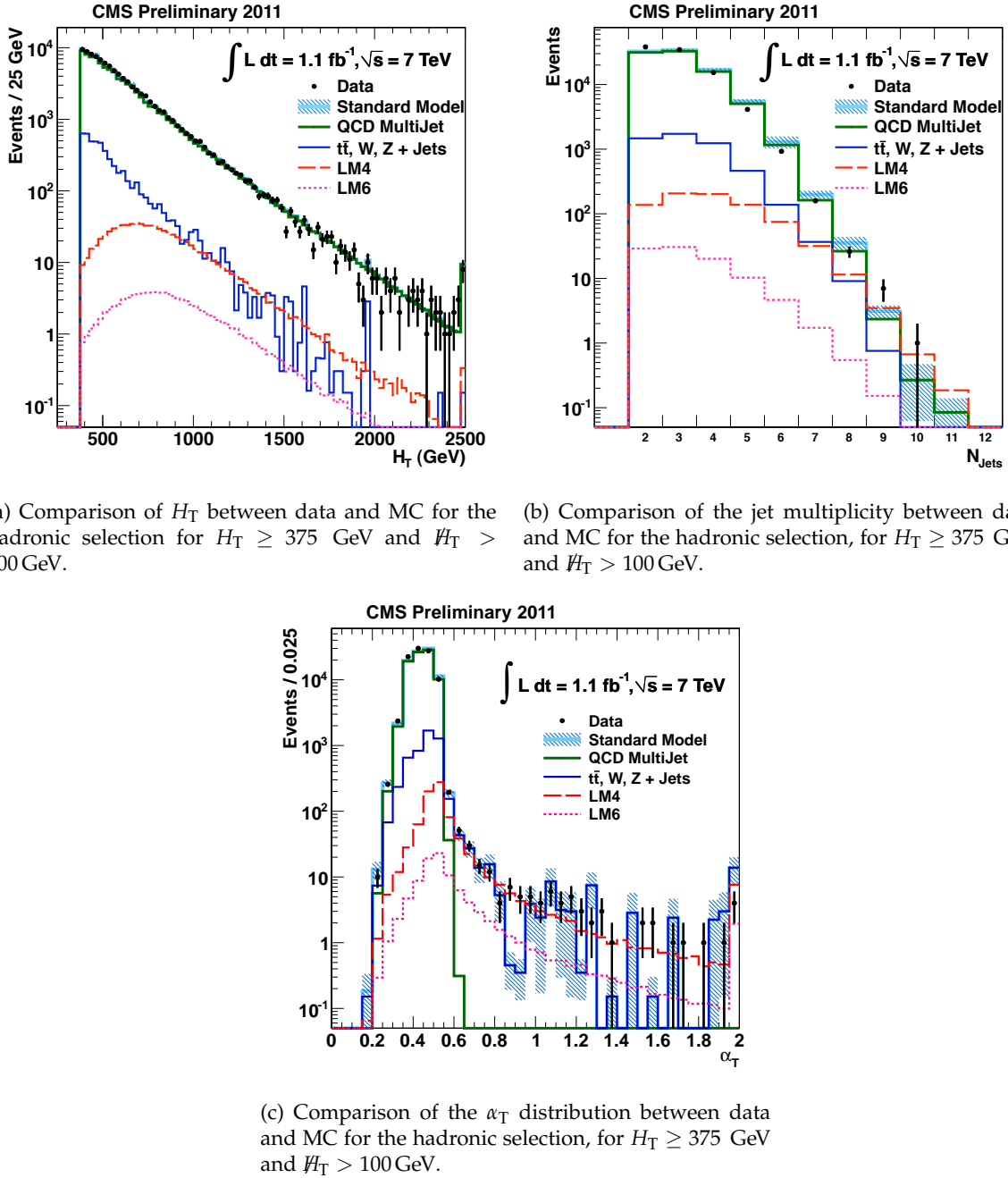
## 2.1 Data to Monte Carlo Comparison for Analysis Variables

In the following we show data–MC comparisons before the  $\alpha_T > 0.55$  selection and requiring  $H_T > 375 \text{ GeV}$  and  $\cancel{H}_T > 100 \text{ GeV}$ , slightly higher than the trigger requirement. The data–MC comparison plots are used to demonstrate the quality of the simulation, but are not used for the background prediction. The actual background yields are obtained from data control samples, as described further below. The uncertainties displayed on the MC distributions only correspond to the statistical uncertainties and do not include systematic uncertainties due to, e.g., jet energy scale or resolution.

Figures 1a and 1b show the comparisons between data and MC simulation for the  $H_T$  variable and the number of reconstructed jets per event, before the requirement on  $\alpha_T$ . Good agreement is observed between data and MC simulation.

Figure 1c shows the  $\alpha_T$  distribution and demonstrates that this variable is an excellent discriminator between QCD background and signal. The number of expected QCD events quickly falls to zero with increasing  $\alpha_T$ .

Figures 2a, 2b and 2c show comparisons between simulated standard model distributions and data for events passing the  $\alpha_T$  selection. The  $\Delta\phi^*$  distribution in Figure 2a shows an approximately flat behaviour as expected from SM processes with real missing transverse energy such as  $t\bar{t}$ ,  $W + \text{jets}$  and  $Z \rightarrow \nu\bar{\nu} + \text{jets}$  events. No evidence for QCD multi-jet events which would peak at small values of  $\Delta\phi^*$  is seen. Generally, the observed distributions in data show no deviation from the standard model prediction.

Figure 1: Comparisons of basic quantities before the  $\alpha_T$  selection cuts.

## 2.2 $H_T$ Dependence of $R_{\alpha_T}$

The ratio  $R_{\alpha_T} = N^{\alpha_T > \theta} / N^{\alpha_T < \theta}$  exhibits no dependence on  $H_T$  if  $\theta$  is chosen such that the numerator of the ratio in all  $H_T$  bins is dominated by  $t\bar{t}$ ,  $W$  + jets and  $Z \rightarrow \nu\bar{\nu}$  + jets events (referred to in the following as EWK) and there is no significant contribution from events from QCD multi-jet production [1]. This is demonstrated in Figure 3, using MC simulations for the cut value  $\theta = 0.55$  over the range  $275 < H_T < 975$  GeV.

One important ingredient in the  $R_{\alpha_T}$  method is the scaling of the jet  $p_T$  thresholds in the low  $H_T$  bins to maintain jet multiplicities and thus comparable event kinematics and topologies in the different  $H_T$  bins. This is especially important in the case of the  $t\bar{t}$  background, which have on

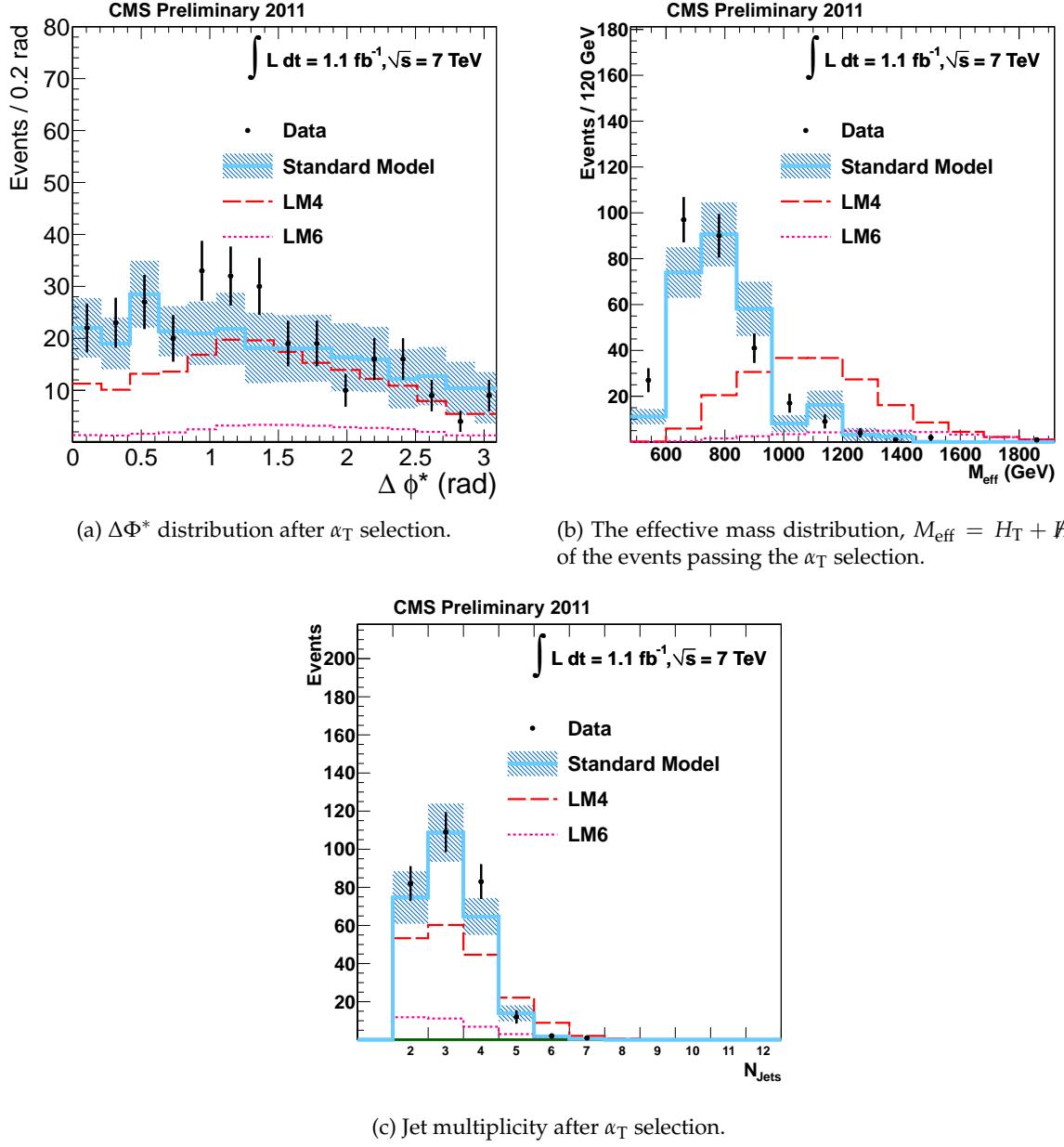


Figure 2: Comparisons between data and MC after the  $\alpha_T$  selection cut.

average a higher jet multiplicity than the other EWK backgrounds. If the jet  $p_T$  thresholds were not scaled relative to  $H_T$  in the lowest  $H_T$  bins,  $t\bar{t}$  events would exhibit a turn-on behaviour at low  $H_T$  before falling off exponentially like the other SM backgrounds at high  $H_T$ . Thus, in accordance with the 2010 analysis, the jet  $p_T$  thresholds are scaled only for the first two  $H_T$  bins, and remain fixed for all subsequent bins. The thresholds are listed in Table 1.

Figure 3 (left) shows the dependence of  $R_{\alpha_T}$  on  $H_T$ , as measured in data and also obtained from MC simulations of SM, and SM plus the SUSY benchmark points LM4 or LM6. The data (SM expectations) are consistent with the flat hypothesis, with p-values of 0.29 (0.50). The SM+LM4 and SM+LM6 are not consistent with constant  $R_{\alpha_T}(H_T)$ , thus demonstrating that the presences of a SUSY signal would result in a significant deviation from the hypothesis of RaT being flat with  $H_T$ . As will be discussed in more detail in Sec. 4, we also pursue an alternative approach which allows for a small QCD contribution in the low  $H_T$  regions. However, we have found

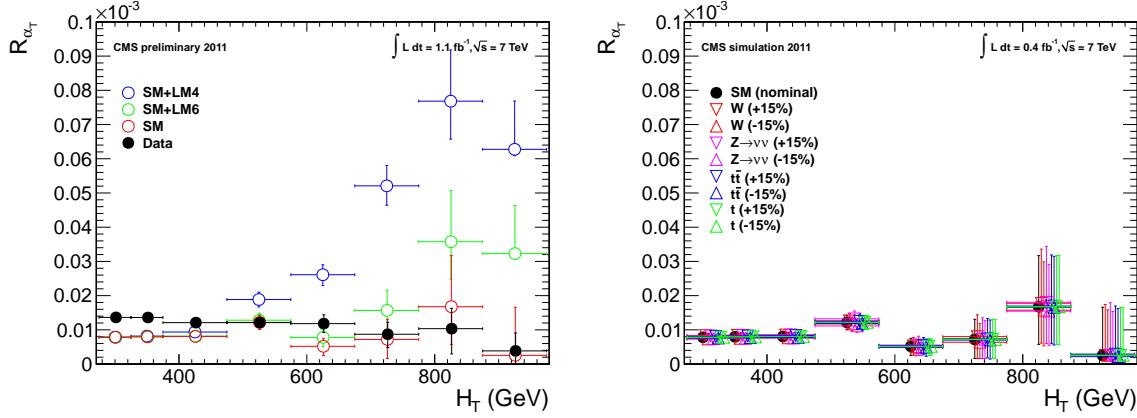


Figure 3: (Left) The dependence of  $R_{\alpha_T}$  on  $H_T$  for events with  $N_{\text{jet}} \geq 2$ . (Right) Dependence of  $R_{\alpha_T}$  on  $H_T$  when varying the effective cross-section of the four major EWK background components individually by  $\pm 15\%$ . (Markers are artificially offset for clarity.)

no evidence in the 2011 data that would invalidate the QCD free hypothesis, which in turn is assumed to lead to  $R_{\alpha_T}$  being constant with  $H_T$ .

Figure 3 (right) demonstrates the independence of  $R_{\alpha_T}$  on  $H_T$ , based on MC simulations, even when varying the effective cross-section of the four major EWK background components individually by as much as  $\pm 15\%$ , which reflects our current knowledge of the cross sections for these backgrounds [15, 16]. In each case, the behaviour is always consistent with the flat hypothesis, with a p-value of at least 0.47. Studies with larger variations of  $\pm 50\%$  also lead to p-values that are consistent with the flat hypothesis. This is how the assumption of flat behaviour is tested against the systematic uncertainties associated with the cross-section measurements of the different EWK backgrounds.

In 2010, a cut-based approach was used, in which an extrapolation from a low- $H_T$  control region ( $250 \text{ GeV} < H_T < 350 \text{ GeV}$ ) into the  $H_T$  signal region ( $H_T > 350 \text{ GeV}$ ) was performed in order to estimate the SM background. In the current analysis of the 2011 data, a shape analysis over the entire  $H_T > 275 \text{ GeV}$  region is carried out.

### 2.3 Estimation of Background from $t\bar{t}$ and $W + \text{Jets}$ Events using a Muon Control Sample

An estimate of the backgrounds from unidentified leptons and hadronic tau decays originating from high- $p_T$   $W$  bosons is obtained through the use of a muon control sample. In this sample we explicitly select  $W$ 's decaying to a muon and a neutrino in the phase-space of the signal. This is performed in the same  $H_T$  bins as for the hadronic signal selection.

All cuts on jet-based quantities are consistent with those applied in the hadronic search region.

In order to select  $W$  events we have the following additional cuts:

- One isolated muon with  $p_T > 10 \text{ GeV}$  and  $|\eta| < 2.5$ .
- $M_T > 30 \text{ GeV}$ , where  $M_T$  is the transverse mass of the  $W$  candidate.
- $\Delta R(\text{jet}, \text{muon}) > 0.5$
- $\cancel{H}_T / H_T > 0.4$
- No second isolated muon in the event. This reduces  $Z \rightarrow \mu\mu$ .

The number of events from  $W$ +jet events in the hadronic selection  $W_{\text{data}}^{\text{had}}$  can be estimated from the event yield,  $W_{\text{data}}^{\mu}$ , of these type of events. This is done using the expected relative ratio of those two types of events. The value of this ratio is extracted from the MC, and thus the estimated number of  $W$  events in the hadronic analysis is calculated by

$$W_{\text{data}}^{\text{had}} = W_{\text{data}}^{\mu} \times \frac{W_{\text{MC}}^{\text{had}}}{W_{\text{MC}}^{\mu}}.$$

In the lowest two  $H_T$  bins, the value of  $\frac{W_{\text{MC}}^{\text{had}}}{W_{\text{MC}}^{\mu}}$  is extracted separately. However, due to low Monte Carlo statistics in the highest  $H_T$  bins, one value for the ratio is used for  $H_T > 375$  GeV. The MC translation factor, which is listed in Table 2, is expected to exhibit only a weak dependence on  $H_T$ . Table 2 shows the split of the muon control sample numbers and the corresponding background prediction in the different  $H_T$  bins. The errors quoted on the predictions correspond to statistical errors and to an additional systematic uncertainty of 30%, as used in the previous analysis [1]. There is good agreement between data and MC, as shown both before (Figure 4) and after (Figure 5) the  $\alpha_T$  cut.

Table 2: Muon sample predictions with  $1.1\text{fb}^{-1}$ . Errors quoted on predictions correspond to statistical errors and an additional conservative systematic uncertainty of 30%, as used in the previous analysis.

$H_T$ Bin (GeV)	275–325	325–375	375–475	475–575
MC $W + t\bar{t}$	$463.0 \pm 16.0_{\text{stat}}$	$171.2 \pm 9.5_{\text{stat}}$	$116.3 \pm 8.3_{\text{stat}}$	$43.7 \pm 5.1_{\text{stat}}$
MC $\mu +$ jets	$407.5 \pm 14.5_{\text{stat}}$	$179.1 \pm 9.6_{\text{stat}}$	$131.6 \pm 8.8_{\text{stat}}$	$48.7 \pm 5.5_{\text{stat}}$
MC Ratio	1.14	0.96	0.90	0.90
Data $\mu +$ jets	389	156	113	39
$W + t\bar{t}$ Prediction	$442.0 \pm 22.4_{\text{stat}} \pm 132.6_{\text{syst}}$	$149.1 \pm 11.9_{\text{stat}} \pm 44.7_{\text{syst}}$	$101.9 \pm 9.6_{\text{stat}} \pm 30.6_{\text{syst}}$	$35.2 \pm 5.6_{\text{stat}} \pm 10.6_{\text{syst}}$
$H_T$ Bin (GeV)	575–675	675–775	775–875	875– $\infty$
MC $W + t\bar{t}$	$17.5 \pm 3.2_{\text{stat}}$	$5.1 \pm 1.8_{\text{stat}}$	$1.1 \pm 0.7_{\text{stat}}$	$1.8 \pm 1.0_{\text{stat}}$
MC $\mu +$ jets	$13.3 \pm 2.9_{\text{stat}}$	$8.0 \pm 2.3_{\text{stat}}$	$3.2 \pm 1.4_{\text{stat}}$	$0.9 \pm 0.7_{\text{stat}}$
MC Ratio	0.90	0.90	0.90	0.90
Data $\mu +$ jets	17	5	0	0
$W + t\bar{t}$ Prediction	$15.3 \pm 3.7_{\text{stat}} \pm 4.6_{\text{syst}}$	$4.5 \pm 2.0_{\text{stat}} \pm 1.4_{\text{syst}}$	$0.0 \pm 1.0_{\text{stat}}$	$0.0 \pm 1.0_{\text{stat}}$

## 2.4 Estimation of Background from $Z \rightarrow \nu\bar{\nu} +$ Jets from Photon + Jets Events

$Z \rightarrow \nu\bar{\nu} +$ jet events form an irreducible background. An estimate of this background can be obtained from the  $\gamma +$  jets process, which has a larger cross section but kinematic properties similar to those of  $Z \rightarrow \nu\bar{\nu}$  events when the photon is ignored (see e.g. [7] and [17]). The  $\gamma +$  jet sample is selected by requiring photons, i.e. localized electromagnetic depositions satisfying tight isolation criteria, with  $p_T$  greater than 100 GeV,  $|\eta|$  less than 1.45 and  $\Delta R(\gamma, \text{jet}) > 1$ . Ignoring the photon, the same hadronic final state selection as in the signal selection is applied.

Table 3 shows the observed counts in the photon control sample and the corresponding background predictions. As in [1], we use a 40% total systematic uncertainty on the method. Figure 6 shows the  $\alpha_T$  and jets multiplicity distributions for the selected photon control sample.

## 2.5 Background Cross-Check: Estimation of $W \rightarrow \mu\nu +$ Jets Events from Photon + Jets Events

To verify that our background estimation method for  $Z \rightarrow \nu\bar{\nu}$  events is performing as expected, and that the assigned systematic uncertainties are adequate, we use the photon + jets sample to

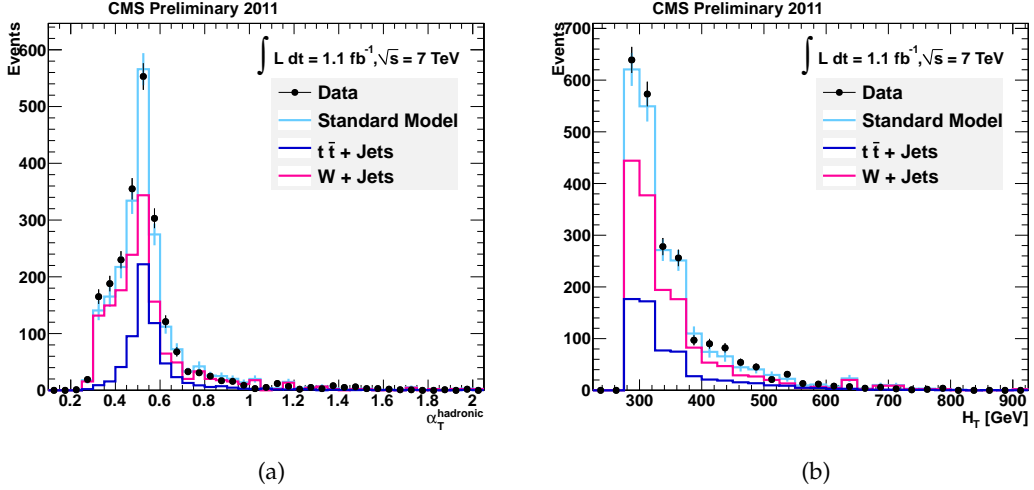


Figure 4: Data - Monte Carlo comparisons for the muon control selection before the  $\alpha_T > 0.55$  cut is applied, shown for (a)  $\alpha_T$  and (b)  $H_T$ . A cut of  $HT > 375$  GeV has been applied, to select the region of fixed jet thresholds.

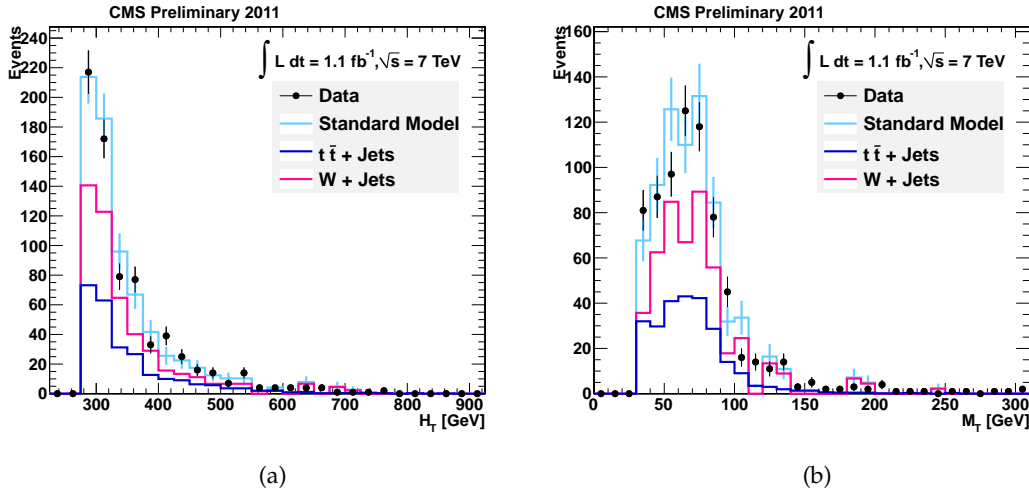


Figure 5: Data - Monte Carlo comparisons for the muon control selection after the  $\alpha_T > 0.55$  cut is applied, shown for (a)  $H_T$  and (b)  $M_T$ . A cut of  $HT > 375$  GeV has been applied, to select the region of fixed jet thresholds.

predict the number of  $W \rightarrow \mu\nu$  events, which is kinematically similar to the process  $Z \rightarrow \nu\bar{\nu} + \text{jets}$ . To reject events originating from  $t\bar{t}$  production, and to obtain a pure  $W + \text{jets}$  sample, the number of jets is limited to two. The number of  $W$  events can then be obtained as follows:

$$N_{\text{data}}^W = N_{\text{data}}^{\text{Phot}} \times \frac{N_{\text{MC}}^W}{N_{\text{MC}}^{\text{Phot}}}.$$

The factor  $\frac{N_{\text{MC}}^W}{N_{\text{MC}}^{\text{Phot}}}$ , which corrects for selection efficiencies and acceptance, is taken from MC simulation. Within the statistical precision of the MC sample, it is found to be approximately independent of  $H_T$ . We thus use a constant factor of  $0.42 \pm 0.04$ . The results are summarized

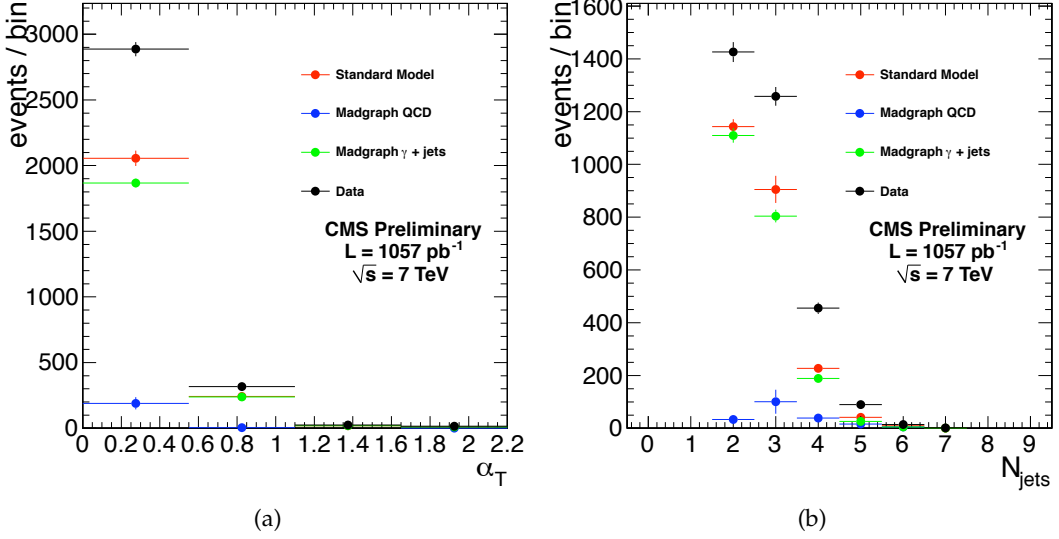


Figure 6: Data-MC comparisons for the photon control sample.  $H_T > 375$  GeV and  $H_T/H_T > 0.4$  are required. Left: the distribution of  $\alpha_T$ . Right: the distribution of the number of jets.

Table 3: Photon Sample Predictions  $1.1\text{fb}^{-1}$

$H_T$ Bin (GeV)	275–325	325–375	375–475	475–575
MC $Z \rightarrow \nu\bar{\nu}$	$212.6 \pm 20.4_{\text{stat}}$	$92.0 \pm 20.4_{\text{stat}}$	$61.3 \pm 20.4_{\text{stat}}$	$42.9 \pm 10.2_{\text{stat}}$
MC $\gamma + \text{jets}$	$613.1 \pm 20.4_{\text{stat}}$	$265.7 \pm 10.2_{\text{stat}}$	$168.6 \pm 10.2_{\text{stat}}$	$55.2 \pm 8.2_{\text{stat}}$
MC Ratio	0.35	0.35	0.44	0.44
Data $\gamma + \text{jets}$	867.5	313.7	214.6	68.5
Sample Purity	0.92	0.97	0.99	0.99
$Z \rightarrow \nu\bar{\nu}$ Prediction	$276.8 \pm 9.5_{\text{stat}} \pm 110.7_{\text{syst}}$	$105.3 \pm 6.0_{\text{stat}} \pm 42.1_{\text{syst}}$	$93.5 \pm 6.4_{\text{stat}} \pm 37.4_{\text{syst}}$	$29.8 \pm 3.6_{\text{stat}} \pm 11.9_{\text{syst}}$
$H_T$ Bin (GeV)	575–675	675–775	775–875	875– $\infty$
MC $Z \rightarrow \nu\bar{\nu}$	$5.1 \pm 5.1_{\text{stat}}$	$0.0 \pm 3.1_{\text{stat}}$	$3.1 \pm 3.1_{\text{stat}}$	$0.0 \pm 3.1_{\text{stat}}$
MC $\gamma + \text{jets}$	$23.5 \pm 5.1_{\text{stat}}$	$3.1 \pm 2.0_{\text{stat}}$	$3.1 \pm 2.0_{\text{stat}}$	$2.0 \pm 1.0_{\text{stat}}$
MC Ratio	0.44	0.44	0.44	0.44
Data $\gamma + \text{jets}$	24.5	12.3	4.1	4.1
Sample Purity	0.99	0.99	0.99	0.99
$Z \rightarrow \nu\bar{\nu}$ Prediction	$10.7 \pm 2.2_{\text{stat}} \pm 4.3_{\text{syst}}$	$5.3 \pm 1.5_{\text{stat}} \pm 2.1_{\text{syst}}$	$1.8 \pm 0.9_{\text{stat}} \pm 0.7_{\text{syst}}$	$1.8 \pm 0.9_{\text{stat}} \pm 0.7_{\text{syst}}$

in Table 4 and the predicted number of muon events is in good agreement with the observed number within the assigned systematic uncertainties.

Table 4: Predictions of  $W + \text{two jets}$  events using the photon sample  $1.1\text{fb}^{-1}$ .

$H_T$	$N_{\text{data}}^{\text{phot}}$	$N_{\text{MC}}^W / N_{\text{MC}}^{\text{phot}}$	$N_{\text{pred}W}^W$	$N_{\text{obs}}^W$
275	336	$0.42 \pm 0.04_{\text{MCstat}}$	$141.8 \pm 7.7_{\text{stat}} \pm 14.6_{\text{MCstat}} \pm 56.7_{\text{syst}}$	128
325	127	$0.42 \pm 0.04_{\text{MCstat}}$	$53.6 \pm 4.8_{\text{stat}} \pm 5.5_{\text{MCstat}} \pm 21.4_{\text{syst}}$	37
375	96	$0.42 \pm 0.04_{\text{MCstat}}$	$40.5 \pm 4.1_{\text{stat}} \pm 4.2_{\text{MCstat}} \pm 16.2_{\text{syst}}$	36
475	27	$0.42 \pm 0.04_{\text{MCstat}}$	$11.4 \pm 2.2_{\text{stat}} \pm 1.2_{\text{MCstat}} \pm 4.6_{\text{syst}}$	12
575	13	$0.42 \pm 0.04_{\text{MCstat}}$	$5.5 \pm 1.5_{\text{stat}} \pm 0.6_{\text{MCstat}} \pm 2.2_{\text{syst}}$	2

### 3 Systematic Uncertainties on Signal Efficiency

The systematic uncertainties on the signal event yield are estimated following in general the recipes discussed in [1] and are split into two parts: theoretical uncertainties on the predicted

cross section of the different production processes (squark-squark, squark-gluino, gluino-gluino) and experimental uncertainties on the integrated luminosity and on the selection efficiency.

The experimental systematic uncertainties on the estimated signal event yield are the uncertainty on the luminosity measurement (6%) [18], the effect of rejecting events with jets pointing to masked ECAL regions (3%) [1], the modelling of the lepton and photon vetoes in the simulation (2.5%) [1], and the effect of the uncertainty in the jet energy scale and resolution on the selection efficiency (2.5%) [1, 19].

The systematic uncertainties on the next-to-leading order (NLO) cross section predictions due to the choice of the renormalization and factorization scales combined with the uncertainties on the used parton distribution functions amount to a 10% systematic uncertainty.

These uncertainties are all included in the limit calculation.

## 4 Framework for Statistical Interpretation

This section outlines the statistical framework used for the limit interpretation of the observed yields of the  $H_T$  shape analysis.

### 4.1 Hadronic Selection

Let  $N$  be the number of  $H_T$  bins. The bins need not have equal width. Let  $n^i$  represent the number of events observed with  $\alpha_T > 0.55$  in each  $H_T$  bin  $i$ . The likelihood of the observations is expressed as:

$$L_{\text{hadronic}} = \prod_i \text{Pois}(n^i | b^i + s^i) \quad (1)$$

where  $b^i$  represents the expected SM background in bin  $i$ , and  $s^i$  represents the expected number of signal events in bin  $i$ .

We assume that  $b^i \equiv \text{EWK}^i + \text{QCD}^i$ , where  $\text{EWK}^i$  is the expected yield of electroweak events in bin  $i$ , and  $\text{QCD}^i$  is the expected yield of QCD events in bin  $i$ . We then model  $R_{\text{QCD}^i}$  as falling exponentially with  $H_T$  and  $R_{\text{EWK}^i}$  as constant across  $H_T$  as described in Section 4.5. We define  $Z_{\text{inv}}^i \equiv f_{\text{Zinv}}^i \times \text{EWK}^i$ , and  $t\bar{t}W^i \equiv (1 - f_{\text{Zinv}}^i) \times \text{EWK}^i$ . The variables  $Z_{\text{inv}}^i$  and  $t\bar{t}W^i$  are used in Section 4.4. Each  $f_{\text{Zinv}}^i$  is a fit parameter, and is limited to be between zero and one.

### 4.2 Testing the Goodness-of-Fit of the SM-only Hypothesis

In Equation 1, we set  $s^i = 0$  for all  $i$ . We determine the set of parameter values which maximizes the likelihood function specified in Section 4.6, and note the corresponding value  $L_{\text{max}}^{\text{data}}$  of the likelihood. The likelihood function (using these parameter values) is then used as a probability density function for the observations to generate many pseudo-experiments. For each pseudo-experiment, we maximize the likelihood function over all parameters, and note the corresponding value  $L_{\text{max}}$ . We determine the quantile of  $L_{\text{max}}^{\text{data}}$  in the resulting distribution of  $L_{\text{max}}$ , and quote the result as a  $p$ -value.

### 4.3 Testing specific SUSY Models

Let  $x$  represent the cross-section for the model in question, and let  $l$  represent the recorded luminosity. Let  $\epsilon_{\text{had}}^i$  be the analysis efficiency as simulated for the model in  $H_T$  bin  $i$ . We take the uncertainty on the efficiency to be fully correlated among the bins. Let  $\delta$  represent the

relative uncertainty on the signal yield in a bin  $i$ . Let  $\rho_{sig}$  represent the “correction factor” to the signal yield which accommodates systematic uncertainties. Let  $f$  be the parameter of interest, for which we shall determine the allowed interval. We write the likelihood of the observations this way:

$$L_{hadronic} = \text{Gaus}(1.0 | \rho_{sig}, \delta) \times \prod_i \text{Pois}(n^i | b^i + f\rho_{sig} xle_{had}^i) \quad (2)$$

If the upper limit of the interval for  $f$  is less than one, then we consider the model incompatible with the data.

#### 4.4 Electroweak Background Constraints

In each bin of  $H_T$ , we have two measurements:  $n_{ph}$ , and  $n_{mu}$ , representing the event counts in the photon and muon control samples. Each of these measurements has a corresponding Monte Carlo expectation:  $MC_{ph}$ , and  $MC_{mu}$ . The Monte Carlo also gives expected amounts of  $Z_{inv}$  and  $t\bar{t} + W$  in the hadronically-selected sample:  $MC_{Z_{inv}}$  and  $MC_{t\bar{t}+W}$ . Let  $i$  label the  $H_T$  bin, let  $\sigma_{phZ}^{inp}$  and  $\sigma_{muW}^{inp}$  represent the relative systematic uncertainties for the control sample constraints. Define

$$r_{ph}^i = \frac{MC_{ph}^i}{MC_{Z_{inv}}^i}; r_{mu}^i = \frac{MC_{mu}^i}{MC_{t\bar{t}+W}^i} \quad (3)$$

We treat the systematics as fully correlated among the  $H_T$  bins. We use this likelihood:

$$L_{ph} = \text{Gaus}(1.0 | \rho_{phZ}, \sigma_{phZ}^{inp}) \times \prod_i \text{Pois}(n_{ph}^i | \rho_{phZ} r_{ph}^i Z_{inv}^i) \quad (4)$$

$$L_{mu} = \text{Gaus}(1.0 | \rho_{muW}, \sigma_{muW}^{inp}) \times \prod_i \text{Pois}(n_{mu}^i | \rho_{muW} r_{mu}^i ttW^i + s_{mu}^i) \quad (5)$$

The parameters  $\rho_{phZ}$  and  $\rho_{muW}$  represent “correction factors” which accommodate systematic uncertainty. The variable  $Z_{inv}^i$  represents the expected number of  $Z \rightarrow \nu\bar{\nu}$  events in  $H_T$  bin  $i$  of the hadronically selected sample. The variable  $ttW^i$  represents the expected number of events from SM  $W$ -boson production (including top quark decays) in  $H_T$  bin  $i$  of the hadronically selected sample.

We define  $s_{mu}^i \equiv f\rho_{sig} xle_{mu}^i$ , where  $\epsilon_{mu}^i$  is the analysis efficiency of the muon-selection on the SUSY model in question in  $H_T$  bin  $i$ , and the other parameters are defined in Section 4.3.

#### 4.5 $H_T$ Evolution Method

The hypothesis that the  $R_{\alpha_T}$  falls exponentially in  $H_T$ :

$$R_{\alpha_T}(H_T) = Ae^{-kH_T} \quad (6)$$

involves the two parameters  $A$  and  $k$  whose values will be determined. A constant ratio is equivalent to requiring  $k = 0$ . Let  $m_i$  represent the number of events observed with  $\alpha_T \leq 0.55$  in each  $H_T$  bin  $i$ . The expected background is written thus:

$$b_i = \int_{x_i}^{x_{i+1}} \frac{dN}{dH_T}(x) A e^{-kx} dx. \quad (7)$$

where  $\frac{dN}{dH_T}$  is the distribution of  $H_T$  for events with  $\alpha_T \leq 0.55$ ,  $x_i$  is the lower edge of the bin, and  $x_{i+1}$  is the upper edge of the bin ( $\infty$  for the final bin). We assume

$$\frac{dN}{dH_T}(x) = m_i \delta(x - \langle H_T \rangle_i), \quad (8)$$

i.e. within a bin the whole distribution occurs at the mean value of  $H_T$  in that bin. Then

$$b_i = \int_{x_i}^{x_{i+1}} m_i \delta(x - \langle H_T \rangle_i) A e^{-kx} dx = m_i A e^{-k \langle H_T \rangle_i}. \quad (9)$$

## 4.6 Likelihood Model

The likelihood function used is the product of the likelihood functions described in the previous sections:

$$L = L_{hadronic} \times L_{mu} \times L_{ph} \quad (10)$$

There are  $6 + N$  nuisance parameters:  $A_{EWK}$ ,  $A_{QCD}$ ,  $k_{QCD}$ ,  $\{f_{Zinv}^i\}$ , as well as the “systematic” variables  $\rho_{phZ}$ ,  $\rho_{muW}$ ,  $\rho_{sig}$ .

## 5 Final Results

In this section we discuss the results of the statistical interpretation of the  $H_T$  dependent yield measurements in the all-hadronic,  $W$ +jet, and Photon+Jet samples. We consider the following scenario: small QCD contamination mainly in the lower  $H_T$  bins described by a single exponential function (see Section 4.2.); and constant  $R_{\alpha_T}$  as a function of  $H_T$  for the dominant EWK background

The  $H_T$  distributions shown in Figure 7a, 7b, and 7c are the result of the simultaneous fit to the  $H_T$  dependent yield in the all-hadronic,  $W$ +jet and photon+jet sample, respectively. A good agreement between the measured  $H_T$  distributions and the best fit is observed in all three distributions, indicating that the number of events found in data is compatible with the SM background expectation predicted by the fit. With a p-value of 0.56, the hypothesis for the  $H_T$  dependences of  $R_{\alpha_T}$  is well reproduced (see Figure 7d). However, both QCD fit parameters,  $A_{QCD} = (1.4 \pm 1.9) \times 10^{-5}$  and  $k_{QCD} = (5.2 \pm 5.6) \times 10^{-3}$ , are compatible with zero indicating that no significant QCD contamination has been observed in the signal region. The fit results are tabulated in Table 5.

We interpret this lack of signal as a limit on the allowed parameter space of the CMSSM. In each point of the parameter space, the SUSY particle spectrum is calculated using SoftSUSY [20], and the signal events are generated at leading order (LO) with PYTHIA 6.4 [21]. NLO cross sections, obtained with the program Prospino [22], are used to calculate the observed and expected exclusion contours. The simulated signal events are re-weighted to match the average number of pile-up events observed in data.

Table 5: Fit Results for  $1.1\text{fb}^{-1}$ . Since the QCD fit parameters are compatible with zero (see text), the listed QCD contributions in this table are also compatible with zero.

$H_T$ Bin (GeV)	275–325	325–375	375–475	475–575
W + $t\bar{t}$ background	363.7	152.2	88.9	28.8
$Z \rightarrow \nu\bar{\nu}$ background	251.4	103.1	86.4	26.6
QCD background	172.4	55.1	26.9	5.0
Total Background	787.4	310.4	202.1	60.4
Data	782	321	196	62
$H_T$ Bin (GeV)	575–675	675–775	775–875	875– $\infty$
W + $t\bar{t}$ background	10.6	3.1	0.6	0.6
$Z \rightarrow \nu\bar{\nu}$ background	8.7	4.3	2.5	2.2
QCD background	1.0	0.2	0.1	0.0
Total Background	20.3	7.7	3.2	2.9
Data	21	6	3	1

Figure 8 shows the observed and expected 95% CL exclusion limits in the  $m_0$ - $m_{1/2}$  plane for  $\tan\beta = 10$  and  $A_0 = 0\text{ GeV}$  calculated with a two-sided profile likelihood method. Squark and gluino masses of 1.25 TeV can be excluded for values of the common scalar mass at the GUT scale  $m_0 < 530\text{ GeV}$ . When calculating the observed limit using the  $\text{CL}_s$  method [23], squark and gluino masses of 1.1 TeV can be excluded for  $m_0 < 500\text{ GeV}$ .

## 6 Summary

In this note we have presented a search for supersymmetry in dijet and multijet events using the  $\alpha_T$  variable. The analysis presents an update of the published paper [1] with some further refinements. The study is currently based on an integrated luminosity of  $1.1\text{ fb}^{-1}$ , corresponding to a factor 30 increase in analysed data compared to the 2010 analysis. The observed  $H_T$  distribution for events with  $\alpha_T > 0.55$  is in good agreement with the SM expectation obtained from data control samples. In the absence of a signal, limits on the allowed parameter space in the CMSSM were set which exceed those set by previous analyses. Squark and gluino masses of 1.1 TeV can be excluded for values of the common scalar mass at the GUT scale  $m_0 < 0.5\text{ TeV}$ .

## References

- [1] CMS Collaboration, “Search for Supersymmetry in pp Collisions at 7 TeV in Events with Jets and Missing Transverse Energy”, *Phys. Lett.* **B698** (2011) 196–218, arXiv:1101.1628. doi:10.1016/j.physletb.2011.03.021.
- [2] G. L. Kane, C. F. Kolda, L. Roszkowski et al., “Study of constrained minimal supersymmetry”, *Phys. Rev.* **D49** (1994) 6173. doi:10.1103/PhysRevD.49.6173.
- [3] A. H. Chamseddine, R. Arnowitt, and P. Nath, “Locally Supersymmetric Grand Unification”, *Phys. Rev. Lett.* **49** (Oct, 1982) 970–974. doi:10.1103/PhysRevLett.49.970.
- [4] CMS Collaboration, “CMS Physics Technical Design Report, Volume II: Physics Performance”, *J. Phys. G: Nucl. Part. Phys.* **34** (2007) 995–1579.
- [5] L. Randall and D. Tucker-Smith, “Dijet Searches for Supersymmetry at the LHC”, *Phys. Rev. Lett.* **101** 221803 (2008).

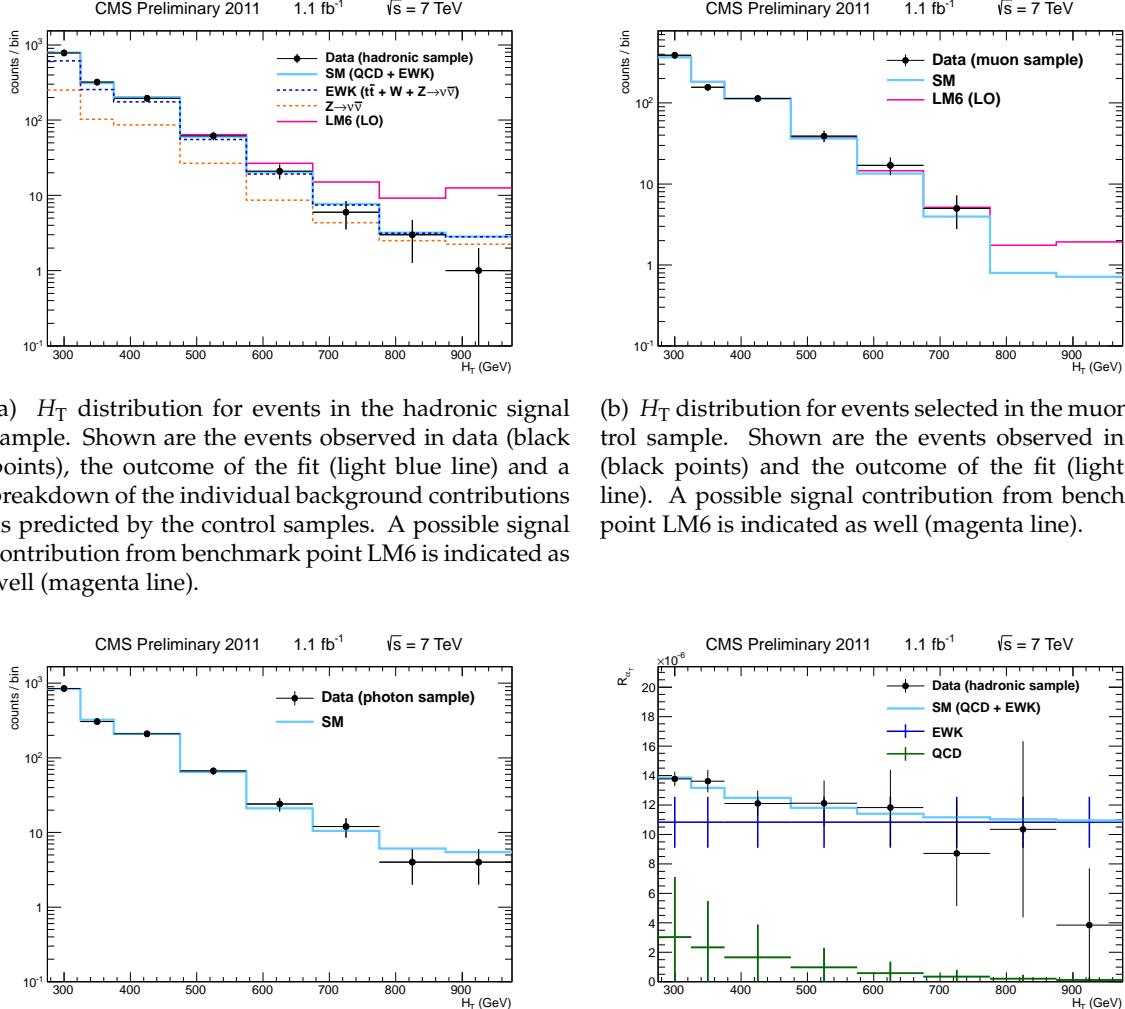


Figure 7: Result of the combined fit to the hadronic, muon and photon samples.

- [6] CMS Physics Analysis Summary, CMS PAS SUS-09-001.
- [7] CMS Physics Analysis Summary, CMS PAS SUS-08-005.
- [8] CMS Collaboration, “Search for New Physics with Jets and Missing Transverse Momentum in pp collisions at  $\sqrt{s} = 7 \text{ TeV}$ ”, [arXiv:1106.4503](https://arxiv.org/abs/1106.4503).
- [9] CMS Collaboration, “Inclusive search for squarks and gluinos in pp collisions at  $\sqrt{s} = 7 \text{ TeV}$ ”, [arXiv:1107.1279](https://arxiv.org/abs/1107.1279).
- [10] M. Cacciari, G. P. Salam, and G. Soyez, “The anti- $k_T$  jet clustering algorithm”, *JHEP* **0804:063** (2008).
- [11] CMS Collaboration, “Calorimeter Jet Quality Criteria for the First CMS Collision Data”, *CMS Physics Analysis Summary JME-09-008* (2009).

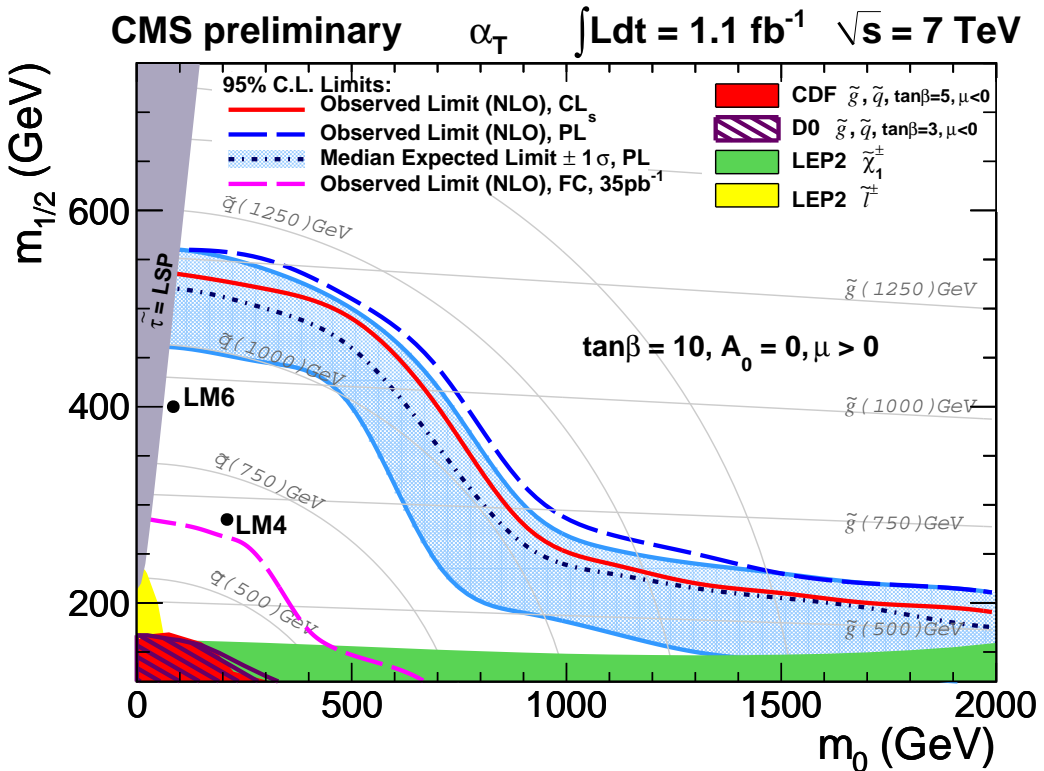


Figure 8: Observed and expected 95% CL exclusion contours in the CMSSM ( $m_0, m_{1/2}$ ) plane ( $\tan\beta = 10, A_0 = 0, \mu > 0$ ) using NLO signal cross sections using the Profile Likelihood (PL) method. The expected limit is shown with its 68% CL range. The observed limit using the  $CL_s$  method is shown as well.

- [12] CMS Collaboration, “Electron reconstruction and identification at  $\sqrt{s} = 7$  TeV”, *CMS Physics Analysis Summary EGM-10-004* (2010).
- [13] CMS Collaboration, “Performance of muon identification in pp collisions at  $\sqrt{s} = 7$  TeV”, *CMS Physics Analysis Summary MUO-10-002* (2010).
- [14] CMS Collaboration, “Photon reconstruction and identification at  $\sqrt{s} = 7$  TeV”, *CMS Physics Analysis Summary EGM-10-005* (2010).
- [15] CMS Physics Analysis Summary, CMS PAS TOP-11-002.
- [16] CMS Physics Analysis Summary, CMS PAS EWK-10-002.
- [17] Z. Bern et al., “Driving Missing Data at Next-to-Leading Order”, [arXiv:1106.1423](https://arxiv.org/abs/1106.1423).
- [18] CMS Collaboration, “Measurement of CMS Luminosity”, *CMS Physics Analysis Summary CMS-PAS-EWK-10-002* (2010).
- [19] CMS Collaboration, “Jet Energy Corrections determination at 7 TeV”, *CMS Physics Analysis Summary JME-10-010* (2010).
- [20] B. C. Allanach, “SOFTSUSY: a program for calculating supersymmetric spectra”, *Comput. Phys. Commun.* **143** (2002) 305. doi:10.1016/S0010-4655(01)00460-X.
- [21] Sjöstrand, Torbjörn and Mrenna, Stephen and Skands, Peter Z., “PYTHIA 6.4 Physics and Manual”, *JHEP* **05** (2006) 026. doi:10.1088/1126-6708/2006/05/026.

- [22] W. Beenakker, R. Hopker, M. Spira et al., “Squark and gluino production at hadron colliders”, *Nucl. Phys.* **B492** (1997) 51–103.  
doi:10.1016/S0550-3213(97)00084-9.
- [23] Particle Data Group Collaboration, “Review of particle physics”, *J. Phys.* **G 37** (2010) 075021. doi:10.1088/0954-3899/37/7A/075021.